PS04: การศึกษาผลการกีดกั้นการส่งผ่านภายในและบริเวณขอบของพลาสมาด้วยวิธีการจำลองในเครื่องปฏิกรณ์ ITER

*ยุทธพงศ์ เพียรโรจน์[1] ธวัชชัย อ่อนจันทร์[1] สุจินต์ สุวรรณะ[1]
รพพน พิชา[2] และ นพพร พูลยรัตน์[3]
[1]หน่วยวิจัยพลาสมา และ ฟิวชัน สถาบันเทคโนโลยีนานาชาติสิรินธร มหาวิทยาลัยธรรมศาสตร์ ต.คลองหนึ่ง อ.คลองหลวง จ.ปทุมธานี 12120
โทรศัพท์ 0 2986 9009, 0 2986 9101 โทรสาร 0 2986 9112-3 E-Mail: yutt_r@yahoo.com
[2]สถาบันเทคโนโลยีนิวเคลียร์แห่งชาติ (องค์การมหาชน)
[3]ภาควิชาฟิสิกส์ มหาวิทยาลัยธรรมศาสตร์ อ.คลองหลวง จ.ปทุมธานี

บทคัดย่อ

การศึกษาผลกระทบการกีดกั้นการส่งผ่านภายในและบริเวณขอบของพลาสมาด้วยวิธีการจำลองในเครื่องปฏิกรณ์อีเทอร์ โดยอาศัยแบบจำลองทางคณิตศาสตร์แบบรวมที่ชื่อ BALDUR เพื่อทำนายผลของอุณหภูมิที่ตำแหน่งสูงสุดของเพเดสทอล (pedestal) สำหรับแบบจำลองที่นำมาใช้ทำนายนั้นตั้งอยู่บนพื้นฐานทางทฤษฎี และมีความกว้างของเพเดสทอล ต่างกันในสามแบบจำลองคือ magnetic and flow shear stabilization ($\Delta \propto \rho_i s^2$), flow shear stabilization ($\Delta \propto \sqrt{\rho_i R q}$), และ normalized poloidal pressure ($\Delta \propto R\sqrt{\beta_{\theta,ped}}$) ในส่วนความกว้างของ pedestal นั้นถูกรวมผลเนื่องจากความแตกต่างของความดันใน ballooning mode รวมกับแบบจำลองการทำนายการส่งผ่านที่บริเวณใจกลางของพลาสมาที่เรียกว่า Mixed Bohm/gyroBohm (Mixed B/gB) โดยรวมผลของการกีดกั้นการส่งผ่านภายใน (Internal Transport Barrier; ITB) แบบจำลองดังกล่าวข้างต้นถูกนำมาใช้เพื่อทำนายลักษณะของพลาสมา และ ประสิทธิภาพของพลาสมาในด้านกำลัง ซึ่งวัดได้จากพารามิเตอร์ Fusion Q โดยพบว่าสำหรับแบบจำลองที่รวมผลการกีดกั้นการส่งผ่านภายในเข้าไป ทำให้ค่า Fusion Q มีค่าสูงขึ้นเมื่อเปรียบเทียบกับกรณีที่ไม่รวมผลการกีดกั้นการส่งผ่านภายใน

คำสำคัญ: เครื่องปฏิกรณ์โทคาแมคอีเทอร์ พลาสมา BALDUR Mixed B/gB

Effect of Internal and Edge Transport Barriers in ITER Simulations

*Y. Pianroj[1], T. Onjun[1], S. Suwanna[1],
[2]R. Picha and [3]N. Poolyyarat
[1]Plasma and Fusion Research Unit, Sirindhorn International Institute of Technology
Thammasat University, Klong Luang, Phathum-Thani, 12120
Phone: 0 2986 9009, 0 29869101, Fax: 0 2986 9112-3, E-Mail: yutt_r@yahoo.com
[2]Thailand Institute of Nuclear Technology (TINT)
[3]Departnent of Physics, Thammasat University, Klong Luang, Phathum-Thani

Abstract

Predictive simulations of ITER with the presence of both an edge transport barrier (ETB) and an internal transport barrier (ITB) are carried out using the BALDUR integrated predictive modeling code. In these simulations, the boundary is taken at the top of the pedestal, where the pedestal values are described using the theory-based pedestal models. These pedestal temperature models are based on three different pedestal width scalings: magnetic and flow shear stabilization ($\Delta \propto \rho_i s^2$), flow shear stabilization ($\Delta \propto \sqrt{\rho_i R q}$), and normalized poloidal pressure ($\Delta \propto R\sqrt{\beta_{\theta,ped}}$). The pedestal width scalings are combined with a pedestal pressure gradient scaling based on ballooning mode limit to predict the pedestal temperature. A version of the semi-empirical Mixed Bohm/gyroBohm (Mixed B/gB) core transport model that includes ITB effects is used to compute the evolution of plasma profiles and plasma performance, which defined by Fusion Q factor. The results from the cases excluding and including ITB are compared. The preliminary results show the Q value resulted from ITB-excluded simulation is less than the one with ITB included.

Keywords: ITER, tokamak, plasma, BALDUR, Mixed B/gB, FusionQ

1. Introduction

The concept of magnetic confinement fusion has long been explored to address the feasibility of nuclear fusion energy. The International Thermonuclear Experimental Reactor (ITER) is an international collaborative effort with the objective of demonstrating the scientific and technological feasibility of nuclear fusion [1]. The goal of ITER is to produce plasmas with a sufficiently high fusion energy density for a long enough time to achieve a sustained fusion burn. Producing a significant fusion reaction rate inside a tokamak requires the ability to heat and contain high-temperature plasmas. Since the high confinement mode (*H*-mode) plasmas in tokamaks generally provide excellent energy confinement and have acceptable particle transport rates for impurity control, fusion experiments such as ITER are designed to operate in the *H*-mode regime. It is known that the improved performance of *H*-mode mainly results from the formation of an edge transport barrier (ETB) [2], called the pedestal. The performance of an *H*-mode discharge can be further improved with the formation of a transport barrier inside the plasma, called an internal transport barrier (ITB) [3]. The presence of both edge and internal transport barriers, results in a complicated scenario that yields higher plasma temperatures and fusion power production. In recent years, predictions of ITER performance in the standard type I ELMy *H*-mode scenario using integrated predictive modeling codes have been intensively studied [4-9]. For example, the BALDUR integrated predictive modeling code with Mixed Bohm/gyroBohm (Mixed B/gB) and MMM95 anomalous core transport models were used to predict the performance of ITER [4, 6-8]. The performance of ITER was evaluated in terms of the fusion power production and the fusion Q, which is the ratio of fusion power (to neutrons and alpha particles) to the applied heating power. A wide range of performance is predicted, depending on the choice of plasma density, heating power, impurity concentration and assumptions about the core transport models employed in the simulations. In the recent work by T Onjun *et al*. [6, 7], the simulations of ITER were carried out with Mixed B/gB and MMM95 core transport model and different ETB models. It was found in all ETB models that the predicted performance of ITER with Mixed B/gB model is relatively low (Fusion $Q \sim 3$) compared to those simulations using MMM95 model (Fusion $Q \sim 10$). It is worth noting that the BALDUR simulations using Mixed B/gB and MMM95 models agree equally well with present-day experiments [10, 11]. A wide range of performance was also found with the Fusion Q of 5-14. In general, the presence of ITBs results in a peaking of plasma profiles in the ITB region. The physics of ITBs can be found in Ref. [3]. There are several models attempting to describe formation of ITBs [13-15]. An original Mixed B/gB model was modified to include the effect of ITBs by suppression of anomalous core transport using $E_r x B$ flow shear and magnetic shear.

In this paper, a study of ITER that includes the effects of ITBs together with the *H*-mode ETB is presented. These simulations are carried out using a BALDUR integrated predictive modeling code, where the ETB is described in terms of a pedestal model since the region considered in these simulations is up to the top of the pedestal. In this work, three best pedestal models in Ref. [22] are chosen. These pedestal models were developed by using the combination of the theoretical-based pedestal width model together with pressure gradient limits imposed by a ballooning mode instability. There are three choices of the pedestal width models considered: magnetic and flow shear stabilization ($\Delta \propto \rho_i s^2$) [17], flow shear stabilization ($\Delta \propto \sqrt{\rho_i R q}$) [16], and normalized poloidal pressure ($\Delta \propto R\sqrt{\beta_{\theta,ped}}$) [18]. These three pedestal temperature models yield similar agreement (with RMSE in the range of 30%) for predicting pedestal temperature when their predictions were compared against type I ELMy *H*-mode discharges from various tokamaks [16]. This pedestal module is taken from the NTCC library [19]. In simulations of discharges that contain an ITB, the ITB is formed by the suppression of core anomalous transport. The Mixed Bohm/gyro-Bohm with ITB effects [14] is used. The presence of both an ITB and an ETB results in complicated scenarios that yield improved performance compared with standard *H*-mode discharges.

2. BALDUR, ITB model and ETB model

The BALDUR integrated predictive modeling code [20] is used to compute the time evolution of plasma profiles including electron and ion temperatures, deuterium and tritium densities, helium and impurity densities, safety factor, neutrals, and fast ions.

In this work, an ITB is formed by the suppression of core anomalous transport due to $\omega_{E\times B}$ flow shear and magnetic shear. This effect is included in the Mixed Bohm/gyro-Bohm (Mixed B/gB) anomalous core transport model [16]. This core transport model is an empirical model. It was originally a local transport model with Bohm scaling. A transport model is said to have “Bohm” scaling when the transport diffusivities are proportional to the gyro-radius times thermal velocity. Transport diffusivities in models with Bohm scaling are also functions of the profile shapes (characterized by normalized gradients) and other plasma parameters, such as magnetic q. These parameters are held fixed in systematic scans in which only the gyro-radius is changed relative to plasma dimensions. The original model was subsequently extended to describe ion transport, and a gyro-Bohm term was added in order to produce simulation results that match data from smaller tokamaks as well as data from larger machines. A transport model is said to have “gyro-Bohm” scaling when the transport diffusivities are proportional to the square of the gyro-radius times thermal velocity divided by a plasma linear dimension such as the major radius. The Bohm contribution to the original model usually dominates over most of the plasma. The gyro-Bohm contribution usually makes its largest contribution in the deep core of the plasma and it plays a significant role only in smaller tokamaks with relatively low heating power and low magnetic field. To include the ITB effect, the Bohm contribution is modified by a cut-off that is a function of magnetic and flow shear. The Mixed Bohm/gyro-Bohm transport model with ITB effect included [16] can be expressed as follows:

$$\chi_e = 1.0\chi_{gB} + 2.0\chi_B \tag{1}$$

$$\chi_i = 0.5\chi_{gB} + 4.0\chi_B + \chi_{neo} \tag{2}$$

$$D_H = [0.3 + 0.7\rho]\frac{\chi_e\chi_i}{\chi_e + \chi_i} \tag{3}$$

$$D_Z = D_H \tag{4}$$

where

$$\chi_{gB} = 5\times10^{-6}\sqrt{T_e}\left|\frac{\nabla T_e}{B_T^2}\right| \tag{5}$$

$$\chi_B = 4\times10^{-5} R\left|\frac{\nabla(n_e T_e)}{n_e B_T}\right| q^2 \left(\frac{T_{e,0.8} - T_{e,1.0}}{T_{e,1.0}}\right) \Theta\left(-0.14 + s - \frac{1.47 C_{ExB}\omega_{E\times B}}{\gamma_{ITG}}\right) \tag{6}$$

In these expressions, the χ_e is the electron diffusivity, χ_i is the ion diffusivity, D_{H} is the particle diffusivity, D_{z} is the impurity diffusivity, χ_{gB} is the gyro-Bohm contribution, χ_B is the Bohm contribution, ρ is normalized minor radius, T_{e} is the local electron temperature in keV, B_T is the toroidal magnetic field, R is the major radius, n_{e} is the local electron density, q is the safety factor, s is the magnetic shear [r (d q / dr) / q], $\omega_{E\times B}$ is the flow shearing rate, C_{ExB} is the constant for shearing rate effect (in most of simulations, C_{ExB}=1), and the γ_{ITG} is the ITG growth rate, estimated as v_{ti}/qR, in which v_{ti} is the ion thermal velocity. The role of impurity transport is very complicated and crucial for burning plasma experiments since it controls impurity behaviour, such as helium ash accumulation. Since the original Mixed B/gB model does not include impurity transport, in this work, it is assumed that the impurity transport is equal to the particle transport. The $\omega_{E\times B}$ shearing rate used for the formation of ITB is calculated as follows:

$$\omega_{ExB} = \left|\frac{RB_\theta^2}{B_T}\frac{\partial(E_r/RB_\theta)}{\partial\psi}\right| \tag{7}$$

where R is the major radius, B_θ and B_T are the poloidal and toroidal magnetic fields, respectively, Ψ is the poloidal flux, and E_r is the radial electric field for the main plasma ions, which is calculated as follows:

$$E_r = \frac{1}{Zen_i}\frac{\partial p_i}{\partial r} - v_\theta B_T + vB_\theta \tag{8}$$

where $\frac{\partial p_i}{\partial r}$ is the pressure gradient, v_θ and v are the poloidal and toroidal velocities, respectively, and, n_i is the ion density, Z is the ion charge number and e the elementary charge. Note that in this work, the toroidal velocity is taken directly from experiment.

In the development of the pedestal temperature models described in reference [16], two ingredients are required the pedestal width (Δ) and the pressure gradient ($\partial p/\partial r$). If the pedestal density (n_{ped}) is known, the temperature at the top of the pedestal (T_{ped}) can be estimated

$$T_{ped} = \frac{1}{2n_{ped}k}\left|\frac{\partial p}{\partial r}\Delta\right| = \frac{\Delta}{2kn_{ped}}\frac{\alpha_c B_T^2}{2\mu_0 Rq^2}. \tag{9}$$

where k is the Boltzmann constant, μ_0 is the permeability of free space, α_c is the normalized critical pressure gradient, B_T is the magnetic field, R is the major radius and q is the safety factor. In this work, three best pedestal temperature models in reference [16] are selected. These pedestal temperature models yield equally satisfactory agreement with the pedestal data from the ITPA Pedestal Database. These pedestal temperature models are based on either the magnetic and flow shear stabilization width scaling ($\Delta \propto \rho_i s^2$), the flow shear stabilization width scaling ($\Delta \propto \sqrt{\rho_i Rq}$), or the normalized poloidal pressure width scaling ($\Delta \propto R\sqrt{\beta_{\theta,ped}}$), where ρ_l is the ion gyro radius, s is the magnetic shear, and $\beta_{\theta,ped}$ is the normalized pedestal pressure. The pedestal pressure gradient calculation is normally complicated and requires a lot of details. For simplicity, the pedestal gradient is assumed to be uniform throughout the pedestal region and the pedestal gradient is limited by the first stability limit of infinite n ballooning mode, so that the normalized critical pressure gradient for the pedestal region is estimated by

$$\alpha_c \equiv -\frac{2\mu_0 Rq^2}{B_T^2}\left(\frac{\partial p}{\partial r}\right)_c = 0.4s\left(1+\kappa_{95}^2(1+5\delta_{95}^2)\right), \tag{10}$$

where κ_{95} is the elongation at the 95% flux surface, and δ_{95} is the triangularity at the 95% flux surface. The further details of these pedestal temperature models can be obtained from reference [16]. It is worth noting that these pedestal temperature models were derived from different pedestal width scalings. The pedestal width constant in each model was chosen to minimize the RMS deviation with 533 experimental data points from 4 large tokamaks obtained from the International Tokamak Physics Activity (ITPA) pedestal database. So, in this work the pedestal models with the chosen width constant in reference [16] are used. These pedestal temperature models include the effect of edge bootstrap current, which has an impact on magnetic shear and safety factor. This inclusion results in a non-linear behavior in the pedestal temperature model. The scheme to deal with the approximation of magnetic shear and safety factor for the pedestal prediction using the pedestal models was completely described in reference [16]. Therefore, the values of magnetic shear and safety factor for the pedestal calculation are different from the rest of both values in the BALDUR code, which is based on more appropriate calculation. The attempt to use self-consistent safety factor and magnetic shear for all calculations in BALDUR code is underdevelopment. A preliminary result can be seen in Ref. [21]. In addition, there are several new approaches to estimate pedestal values; such as the pedestal scaling by M. Sugihara [12], which predicted the pedestal temperature about 5.6 keV. The pedestal density is described by a simple empirical model. Since the pedestal density, n_{ped}, is usually a large fraction of line average density, n_l, the pedestal density can be calculated as

$$n_{ped} = 0.71 n_l . \qquad (11)$$

This pedestal density model agrees with the pedestal data obtained from the ITPA pedestal database with 12% RMSE [4].

3. Simulation Results and Discussion

The BALDUR code is used to carry out simulations of ITER with the design parameters for full-current standard type I ELMy *H*-mode discharges (R = 6.2 m, a = 2.0 m, I_p = 15 MA, B_T = 5.3 T, κ_{95} = 1.7, δ_{95} = 0.33 and n_l = 1.0x10^{20} m^{-3}). In the simulations, the plasma current and density are slowly ramped up to the target values within the first 100 seconds of the simulation, shown in figure 1. The plasma current during the startup phase is initially 3 MA and is slowly increased at the rate of 0.12 MA/sec to the target current. It is found, using the pedestal module [19], that the plasma makes a transition to the *H*-mode phase at 4 sec during this startup ramp. In this work, the threshold for the transition from *L*-mode to *H*-mode occurs when the plasma heating power exceeds the following empirical expression for the threshold power, taken from [22]:

$$P_{L\to H}\left[MW\right]=2.84M_{AMU}^{-1}B_{T}^{0.82}n_{e,20}^{-0.58}R^{1.00}a^{0.81}. \tag{12}$$

It is worth noting that there are several physical processes that have not been included in these simulations, such as ELM crashes and neoclassical tearing modes. Consequently, the simulation results do not represent the complete dynamic behavior of the ITER plasma. However, it is expected that these simulations include enough physics to describe the plasma when it reaches a quasi-steady state with sawtooth oscillations. The simulations yield complex and interesting interactions within the plasma itself such as the self heating of the plasma by the production of fast alpha particles and redistribution of heating power after each sawtooth crash. Sawtooth oscillations are considered during the simulations. For each simulation, anomalous transport is calculated using the Mixed B/gB transport model with the effect of ITB included, while neoclassical transport is computed using the NCLASS module [23]. The boundary conditions are provided at the top of the pedestal by the pedestal model. In many experiments, it was found that ion pedestal temperature tends to be higher than electron pedestal temperature, especially at low density plasma. Since the ITER plasma is high density plasma, the ion pedestal temperature should not be much different from the electron pedestal temperature. For simplicity, it is assumed in this work that the electron and ion pedestal temperatures have the same values. Note that this assumption was employed in the BALDUR code to carry out the *H*-mode simulations for present day experiments, which the agreement between simulations and experiments was in the range of 10% RMS deviation [4].

In these simulations, the total auxiliary heating power is 40 MW, which is a combination of 33 MW NBI heating power together with 7 MW of RF heating power. As noted above, the Porcelli sawtooth model [24] is used to trigger sawtooth crashes and a modified Kadomtsev magnetic reconnection model [25] is used to compute the effects of each sawtooth crash. Note that during each sawtooth crash, it is assumed that 10% of magnetic flux is mixed to describe the effect of sawtooth crash. During the slow current ramp up phase (reaching the target value in 100 sec), the plasma density is also ramped up to the final plasma density while the full auxiliary heating power is applied starting from the beginning of the simulations that show in Fig 1. During this ramp, the plasma makes an automatic transition from *L*-mode to *H*-mode since the heating power exceeds the power threshold for *L*-*H* transition. Since there is a strong heating early in the simulations, all the simulations enter the *H*-mode phase within approximately 4 sec. The $\omega_{E\times B}$ profile for initiating a formation of an ITB is calculated using Eq. (7). The profile for toroidal velocity is taken directly from one of the Joint European Torus (JET) experiment. In Fig 2, the toroidal velocity profile for an optimized magnetic shear (OS) discharge in JET experiment, discharge 40542 and the calculated $\omega_{E\times B}$ profile using Eq.(7) are shown.

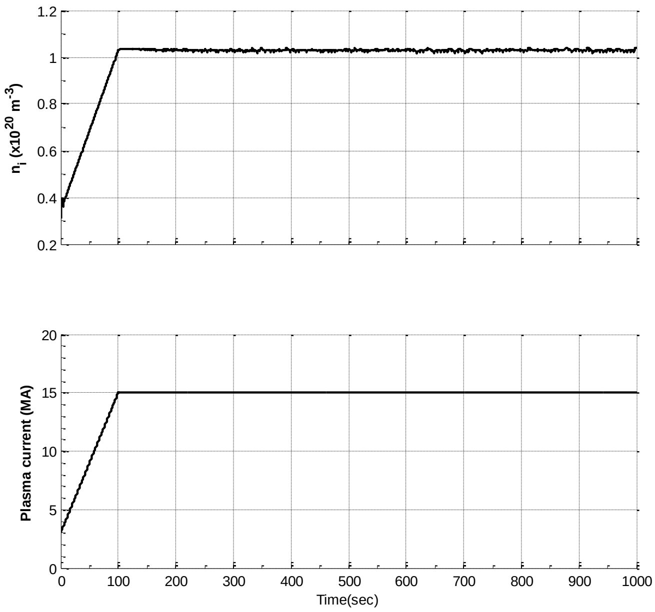

Fig 1: The time evolution of line average density (top) and plasma current (bottom) are shown.

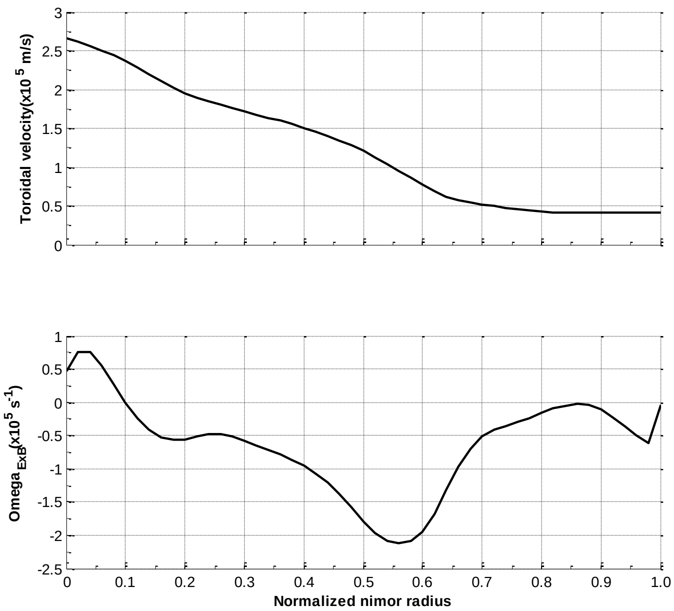

Fig 2: The toroidal velocity (top) and $\omega_{E\times B}$ (bottom) profiles used in this work are plotted as a function of a normalized minor radius. Toroidal velocity profile is taken from JET experiment (discharge 40542), while the $\omega_{E\times B}$ is calculated using Eqs. 6 and 7.

Summaries of the temperatures and densities at the center and at the top of the pedestal predicted by these simulations are shown in Table 1.

Table 1: Summary of electron and ion temperatures, electron density at the time before a sawtooth crash

Parameters	$\Delta\alpha\rho s^2$		$\Delta\alpha\sqrt{\rho R q}$		$\Delta\alpha R\sqrt{\beta_{\theta,ped}}$	
	ITB excluded	ITB included	ITB excluded	ITB included	ITB excluded	ITB included
$T_{i,0}$ (keV)	12.3	35.1	11.8	35.0	13.0	41.4
$T_{e,0}$ (keV)	13.8	33.2	13.3	33.7	14.7	34.0
$n_{e,0}$ (x10^{20} m^{-3})	1.1	1.1	1.1	1.1	1.1	1.1
T_{ped} (keV)	2.6	2.6	2.5	2.5	2.9	2.9
$n_{e,ped}$ (x10^{20} m^{-3})	0.7	0.7	0.7	0.7	0.7	0.7

It can be seen that the central ion temperature increases significantly when the ITB effects are included. For example, the central ion temperatures in the ITB simulation range from 35.0 keV to 41.4 keV. The central ion and electron temperatures in the simulation using the pedestal temperature based on magnetic and flow shear stabilization increase by 190% and 140%, respectively, when simulations with ITB effects are compared with simulations without ITB effects. Note the results for different pedestal temperature models yield the same range of improvement. This increase of central temperature has a strong impact on the total plasma stored energy and the nuclear fusion power production. It can be seen from Table 1 that the pedestal temperature ranges from 2.5 keV to 2.9 keV, which is the expected range for a pedestal in ITER. It is worth noting that these pedestal temperature models are based on first stability limit of infinite n ballooning modes. If the access to the second stability of ballooning modes is included, the predicted pedestal temperature should be significantly higher. In Ref. [5], access to second stability of ballooning mode was found, and consequently the pedestal temperature is close to 5 keV. Therefore, the results obtained in this work can be considered as a minimum projection of ITER performance. It can be seen that the alpha power from the simulation with ITB effects included is much higher than that without an ITB. The average of alpha power during the time between 950 sec and 1000 sec is summarized in Table 2.

Table 2: Summary of average alpha power and Fusion Q during the last 50 sec of the simulations (from 950 sec to 1000 sec).

Parameters	$\Delta\alpha\rho s^2$		$\Delta\alpha\sqrt{\rho Rq}$		$\Delta\alpha R\sqrt{\beta_{\theta,ped}}$	
	ITB excluded	ITB included	ITB excluded	ITB included	ITB excluded	ITB included
$P_{\alpha,\text{avg}}$ [MW]	27.9	164.9	24.1	160.6	32.5	179.6
Fusion Q_{avg}	3.4	20.6	3.0	20.1	4.1	22.4

The fusion performance can be evaluated in term of the Fusion Q, which can be calculated as

$$\text{Fusion } Q = \frac{5 \times P_{\alpha,avg}}{P_{\text{AUX}}}$$

where $P_{\alpha,\text{avg}}$ is a time-average of the alpha power and P_{AUX} is the auxiliary heating power (equal to 40 MW for these simulations). It can be seen in Table 2 that the fusion Q ranges from 20.1 to 22.4 when ITB effects are included. This means that the fusion Q increases by 500%, 570%, and 450% when ITB effects are included in the simulations using the pedestal temperature model based on magnetic and flow shear stabilization, flow stabilization, and normalized poloidal pressure, respectively. The increasing alpha power results in the improved fusion performance that meets the requirement of ITER fusion performance. Note that desired Fusion Q in ITER is equal to 10. It was found in Ref. [9] that the ITER hybrid scenario simulations yielded the fusion Q ranging from 4.2 to 16.1. The plasma current in those simulations in the range of 11 MA to 13 MA, which is lower than that used in the simulations in this work, was used.

4. Summary

Self-consistent simulations of ITER with the presence of both ETB and ITB are carried out using BALDUR code. The combination of Mixed B/gB transport model together with three different pedestal models is used to simulate the time evolution of plasma current, temperature, and density profiles for ITER standard type I ELMy *H*-mode discharges. It is found that ITER fusion performance using BALDUR code with Mixed B/gB transport model without the presence of ITB is quite pessimistic (Fusion $Q \sim 3$). The presence of ITB is crucial and can result in a significant improvement, which is needed for achieving a target Fusion Q of 10. The improvement due to the presence of ITB is almost the same for all simulations with those three pedestal temperature models.

6. Acknowledgments

This project is a part of "Plasma and Fusion Research Unit (PFRU)" and Y. Pianroj would like to thank the Commission on Higher Education, Thailand for supporting by grant fund under the program Strategic Scholarships for Frontier Research Network for the Ph.D. Program Thai Doctoral degree for this research.

7. References

1 Aymar, R. et al., 2002. The ITER Design. Plasma Phys. Control. Fusion 44, 519.

2 Hubbard, A., 2000. Physics and scaling of the H-mode pedestal. Plasma Phys. Control. Fusion 42A, 15.

3 Connor, J. W. et al., 2004. A review of internal transport barrier physics for steady-state operation of tokamaks. Nucl. Fusion 44, R1.

4 Bateman, G. et al., 2003. Integrated predictive modelling simulations of burning plasma experiment designs. Plasma Phys. Control. Fusion 45, 1939.

5 Onjun, T. et al., 2005. Magnetohydrodynamic-calibrated edge-localized mode model in simulations of international thermonuclear experiment reactor. Phys. Plasmas 12, 082513.

6 Onjun, T. et al., 2008. Projected performance of ITER based on different theoretical based pedestal temperature models. Journal of Physics: Conference Series 123, 012034.

7 Tharasrisuthi, K. et al., 2008. Projections of ITER performance based on different pedestal temperature scalings. Thammasat International Journal of Science and Technology 13, 45.

8 Picha, R. et al., 2008. Proceedings from 35th EPS Conf on Plasma Physics, Hersonissos, Greece, 9-13 June 2008.

9 Roach, C. M. et al., 2008. The 2008 Public Release of the International Multi-tokamak Confinement Profile Database. Nucl. Fusion 48, 125001.

10 Hannum, D. et al., 2001. Comparison of high-mode predictive simulation using Mixed Bohm/gyro-Bohm and Multi-Mode (MMM95) transport models. Phys. Plasmas 8, 964.

11 Onjun, T. et al., 2001. Comparison of low confinement mode transport simulations using the mixed Bohm/gyro-Bohm and the Multi-Mode-95 transport model. Phys. Plasmas 8, 975.

12 Zhu, P. et al., 2000. Predictive transport simulation of internal transport barriers using the Multi-Mode model. Phys. Plasmas 7, 2898.

13 Tala, T. J. J. et al., 2001. ITB formation in terms of $\omega_{E\times B}$ flow shear and magnetic shear s on JET. Plasma Phys. Control. Fusion 43, 507.

14 Kinsey, J. E. et al., 2005. Predicting core and edge transport barriers in tokamaks using the GLF23 drift-wave transport model. Phys. Plasmas 12, 052503.

15 Parail, V. V. et al., 1999. Nucl. Fusion 38, 429.